Pediatric RESEARCH

www.nature.com/pr

BASIC SCIENCE ARTICLE

Maternal nutrient restriction in guinea pigs leads to fetal growth restriction with increased brain apoptosis

Andrew Ghaly[1], Yohei Maki[1], Karen Nygard[1], Robert Hammond[1], Daniel B. Hardy[1] and Bryan S. Richardson[1]

BACKGROUND: We determined whether maternal nutrient restriction (MNR) in guinea pigs leading to fetal growth restriction (FGR) impacts cell death in the brain with implications for neurodevelopmental adversity.

METHODS: Guinea pigs were fed ad libitum (Control) or 70% of the control diet before pregnancy, switching to 90% at mid-pregnancy (MNR). Fetuses were necropsied near term and brain tissues processed for necrosis (H&E), apoptosis (TUNEL), and pro- (Bax) and anti- (Bcl-2 and Grp78) apoptotic protein immunoreactivity.

RESULTS: FGR-MNR fetal and brain weights were decreased 38% and 12%, respectively, indicating brain sparing but with brains still smaller. While necrosis remained unchanged, apoptosis was increased in the white matter and hippocampus in the FGR brains, and control and FGR-related apoptosis were increased in males for most brain areas. Bax was increased in the CA4 and Bcl-2 was decreased in the dentate gyrus in the FGR brains supporting a role in the increased apoptosis, while Grp78 was increased in the FGR females, possibly contributing to the sex-related differences.

CONCLUSIONS: MNR-induced FGR results in increased brain apoptosis with regional and sex-related differences that may contribute to the reduction in brain area size reported clinically and increased risk in FGR males for later neurodevelopmental adversity.

Pediatric Research (2019) 85:105–112; https://doi.org/10.1038/s41390-018-0230-6

INTRODUCTION

Epidemiologic studies show that fetal growth restriction (FGR) can impact brain structure and risk for neurodevelopmental adversity. This includes smaller head circumference, reduced brain volumes including hippocampal, and altered neuronal connectivity/delayed myelination in FGR offspring compared to those born appropriate for gestational age (AGA).[1,2] These structural alterations have been associated with deficits in motor skills, cognition, memory and academic ability, and neuropsychological dysfunctions with poor attention and hyperactivity.[1,2] These human studies suggest that critical alterations in brain development arise from the suboptimal conditions that lead to FGR and underlie the risk for later neurological adversities. Since these neurological adversities often relate to memory and learning, hippocampal and associated areas of the nervous system may be particularly vulnerable.[1,2]

FGR remains prevalent in developed countries where placental insufficiency is a major cause and in developing countries where maternal undernourishment plays a greater role.[1–3] However, human studies of FGR and later neurological adversity usually do not take causative factors for FGR into account, assuming since these are mostly from developed countries that placental insufficiency is implicated.[1,2] Nonetheless, global reduction in nutrition during pregnancy leading to FGR can also result in neurological adversities,[4] and maternal undernourishment is still an issue in developed countries.[5]

FGR has been induced in several animal species to provide insight into the brain's developmental adaptations and mechanisms whereby growth alterations occur prenatal and longer term into adulthood.[1,6,7] Much of this study has involved models of placental insufficiency induced by mid-pregnancy or later uterine artery ligation/ablation or placental embolization with hypoxemia through the latter part of pregnancy.[1,6,7] While representing late onset FGR in humans, these vascular models can result in an initial sudden decrease in fetal oxygen delivery relative to consumption contributing to an increased demise rate and possibly to the brain injury in FGR survivors.[1,6–10] Furthermore, there has been limited study in the FGR brain of cell death as a factor in the reduction in brain volumes,[1,6,7] and of sex differences despite the likelihood that brain development will be impacted by sex,[11] and the finding that males are at greater risk for neurodevelopmental adversity.[1,12]

Guinea pigs deliver precocial young with many developmental events occurring during fetal life similar to that in humans.[13] Accordingly, moderate maternal nutrient restriction (MNR) in guinea pigs at 70% of an ad libitum diet preconception until mid-pregnancy increasing to 90% thereafter has been utilized for inducing FGR and studying fetal growth and developmental outcomes. We[10,14] and others[15,16] have shown that this experimental paradigm leads to moderate/severe FGR with fetal weights decreased by 30–40% near term, associated with aberrant placental development, asymmetrical growth, and evidence of chronic hypoxia in visceral tissues as an important signaling mechanism. Moreover, these FGR-MNR fetuses exhibit reduced brain weights which continues to be evident in FGR-MNR neonates.[10,17] These findings support the utility of this model with many similarities to that in humans with moderate/severe FGR whether resulting from maternal undernourishment or placental insufficiency.[3,18–20]

[1]Departments of Obstetrics and Gynecology, Physiology and Pharmacology, Pediatrics, and Pathology, Children's Health Research Institute, Schulich School of Medicine and Dentistry, The University of Western Ontario, London, ON, Canada
Correspondence: Bryan S. Richardson (brichar1@uwo.ca)

Received: 27 June 2018 Revised: 10 October 2018 Accepted: 13 October 2018
Published online: 12 November 2018

We have therefore used moderate MNR in guinea pigs leading to moderate/severe FGR to test the hypothesis that cell death in the brain will be increased, and more so in hippocampal brain areas indicating heightened vulnerability, and in males indicating sex differences. Necrosis and apoptosis have been assessed as measures of cell death since they appear to be part of a continuum whereby immature neurons and/or milder hypoxic insult are more likely to result in apoptotic death, while terminally differentiated neurons and/or severe hypoxic insult are more likely to result in death by necrosis.[21,22] Bax and Bcl-2 immunoreactivity have additionally been examined as important pro- and anti-apoptotic proteins, respectively, whose balance may determine cellular flux toward or away from apoptosis and underlie regional differences in vulnerability to hypoxic insults.[21] G-protein-coupled receptor 78 (Grp78) expression has also been assessed as a chaperone protein whose production is increased to ameliorate the accumulation of unfolded/misfolded proteins seen with hypoxic-related oxidative stress, which if prolonged can initiate a pro-apoptotic cascade.[23,24]

MATERIALS AND METHODS

Animal cohorts and tissue collection

An established model of moderate MNR in guinea pigs[10,14–16] was used with experimental procedures approved by Western University Animal Use Subcommittee. Feeding rationale, maternal weights and food consumption, and pregnancy outcomes have previously been reported.[10,14] Briefly, sows were assigned to a Control group fed ad libitum or an MNR group fed 70% of the average food intake of the control animals on a per kilogram of body weight basis, from 4 weeks pre-conception until mid-pregnancy increasing to 90% thereafter. This dietary regime resulted in actual food consumption by the MNR animals of ~65 to 70% of that consumed by the Control animals throughout pregnancy.[10] On day 60–61 of pregnancy (term ~68 days), sows were sedated followed by laparotomy and delivery of each of the fetuses. Body and placental weights were obtained from all live-born fetuses along with crown-rump length measurements. Fetuses were considered to be AGA if ≥80 g and FGR if <80 g in accordance with weight criteria we[25] and others[26] have used for categorizing AGA and FGR fetal weights in guinea pigs near term. AGA fetuses from Control litters and FGR fetuses from MNR litters were subjected to full necropsy which included weighing of the brain and coronal sectioning at the level of the optic chiasm and through the mammillary body. The rostral and middle brain tissue blocks that included the rostral and mid cortex/subcortex were prepared for histological analysis. The caudal brain tissue block that included the caudal cerebral cortex/subcortex, cerebellum, and brainstem, was fast frozen in liquid nitrogen and stored at −80 °C for protein analysis by western blot.

Eighteen AGA-Control fetuses and 18 FGR-MNR fetuses (each 9 male and 9 female) were selected for brain tissue analysis. These animals were representative of the mean fetal weights for their respective cohort groups and were selected on the basis of no more than one male and one female from each litter.

Histological sample preparation

Tissue blocks for histochemical analyses were immersion fixed in 4% paraformaldehyde for 72 h, washed in phosphate buffered saline (PBS) for 3 days, and then placed in 70% ethanol for 14–21 days. They were then processed to paraffin wax, embedded, sectioned at a thickness of 5 µm on a rotary microtome, and mounted on Superfrost Plus slides (VWR Scientific, Westchester, PA).

Prior to staining, all slides were deparaffinized with three 5-min washes in xylene and then rehydrated in a series of ethanol baths (100, 100, 90, 90, and 70%) lasting 2 min each. Tissue sections were then rinsed in deionized water for 5 min. For all histological staining, all slides for each parameter studied were stained on the same day using the same solutions to minimize variation in intensity of stain.

Haematoxylin and eosin (H&E) stain for necrosis analysis

Neuronal necrosis was assessed using H&E staining. Brain tissue sections were processed as described, then immersed in Harris Modified Haematoxylin (Fisher Scientific, Toronto, ON) for 10 s. The stain was differentiated in 1% acid ethanol for ~1 s and then flushed with running water for 1 min. Tissue sections were then stained with eosin (Fisher Scientific) for ~1 s, followed by dehydration in a series of ethanol baths (70, 70, 90, 100 and 100%), three 5-min washes in xylene, and mounting with Permount (Fisher Scientific).

TUNEL stain for apoptosis analysis

Apoptotic cell injury was assessed by the presence of DNA fragmentation within cells using the TUNEL assay method (Apoptag Peroxidase In Situ Apoptosis Detection Kit; Millipore, Billerica, MA). Tissue sections were processed as described, equilibrated in PBS for 5 min, followed by incubation with proteinase K (20 µg/mL) for 20 min at room temperature, then rinsed four times for 1 min in deionized water. All incubation steps were performed in a covered humidified chamber under plastic coverslips. Positive control slides were generated by equilibrating sections in DN buffer (30 mM Tris/4 mM $MgCl_2$/0.1 mM Dithiothreitol, pH 7.2) for 5 min followed by incubation in 1:25 DNAse 1 (Sigma D7291 Sigma-Aldrich; Oakville, ON) in DN buffer for 10 min, then rinsing four times for 1 min in deionized water.

All slides were quenched with 3% hydrogen peroxide in methanol for 10 min, washed in running water for 5 min, then rinsed in deionized water for 1–2 min. Tissue sections were incubated in equilibration buffer for 30 min, then incubated with terminal deoxynucleotidyl transferase (TdT) enzyme at 37 °C for 1 h. Negative control slides were generated via omission of TdT enzyme with and without DNAse 1. The TdT reaction was stopped with a 10-min rinse in dilute Stop/Wash buffer. Slides were then rinsed three times in PBS and incubated with peroxidase-conjugated antidigoxigenin (DIG) antibody for 30 min. Following four 2-min washes in PBS, a peroxidase substrate (Cardassian Diaminobenzidine (DAB), Biocare Medical; Concord, CA) was applied and developed for 2 min. Sections were rinsed 5 min in running water, counterstained in 50% Harris modified Haematoxylin (Fisher Scientific), then rinsed, dehydrated, cleared, and coverslipped as described for H&E staining.

Bax and Bcl-2 immunohistochemistry (IHC)

IHC for Bax and Bcl-2 was performed using an ImmPRESS anti-rabbit Reagent Kit (Vector Laboratories, Burlingame, CA). Washes were performed in PBS buffer (Thermo-Fisher, Mississauga, ON). Tissue sections were processed as described, incubated in 3.0% hydrogen peroxide for 10 min then blocked for 30 min with 2.5% normal horse serum. Sections were incubated overnight at 4 °C with primary antibody; Bax antibody (1:400; P-19, sc-526, Santa Cruz Biotechnology Inc. Dallas, TX) or Bcl-2 antibody (1:150; AP13823c, Abgent, San Diego, CA). They were then washed and incubated for 40 min with secondary antibody/peroxidase polymer. Bound antibody was visualized with SIGMAFAST 3, 3′-diaminobenzidine (DAB) substrate for 6 min. Sections were counterstained with hematoxylin and mounted as previously described. Preimmune rabbit serum was substituted for primary antibody to generate negative controls.

Imaging and analysis

Analyses were carried out in coronal sections at the level of the optic chiasm and mammillary bodies. Brain regions analyzed included the gray matter layers 2–3 and layers 4–5, and periventricular white matter from both sections, with 12 high-

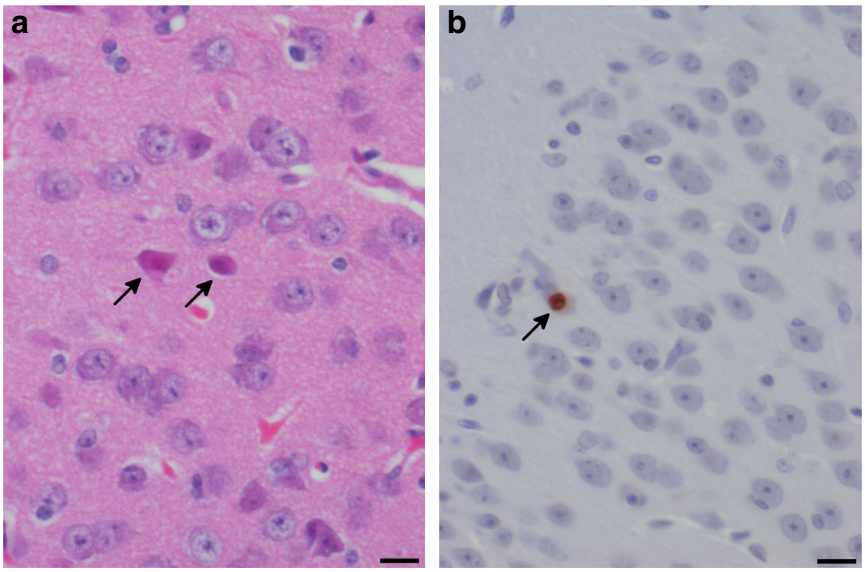

Fig. 1 Photomicrographs of necrotic cells (arrows) in the gray matter of an FGR-MNR fetus (**a**) with hyper-eosinophilic cytoplasm, concave cell profiles, and loss of nuclear detail (haematoxylin and eosin, scale bar = 20μm), and of TUNEL positive cell (arrow) in the gray matter of an FGR-MNR fetus (**b**) (diaminobenzidine/peroxidase, scale bar = 20μm). FGR fetal growth restriction, MNR maternal nutrient restriction

power fields (HPFs) (×40) each; and the hippocampal CA1, CA4, and dentate gyrus, and the thalamus from the section through the mammillary bodies with 6–8 HPFs each. All imaging was performed on a Zeiss AxioImager Z1 microscope (Carl Zeiss Canada Ltd, North York, ON) using a ×40 oil objective. Identical illumination settings were used for all brain regions and analysis was performed using Image Pro Premier 9.2 software (Media Cybernetics Inc., Rockville, MD), with the analyst blinded as to animal group.

Neuronal necrosis was identified with H&E staining by the presence of hyper-eosinophilic cytoplasm, a concave cell profile and a loss of nuclear detail (Fig. 1). Each HPF was scored on a 5-point scale based on the estimated percentage of necrotic-appearing cells, with 0 = 0%, 5 = 1–10%, 30 = 11–50%, 70 = 51–90%, and 95 = 91–100% necrotic cells.[27] Apoptotic cells were identified in TUNEL-stained slides as cells with 3,3′-diaminobenzidine-stained nuclei (Fig. 1). Thresholds were set to identify expression in the positive control slides, while specificity was confirmed by the absence of signal in the negative control slides. For Bax and Bcl-2 immunostained slides, a binary color threshold was set for cell counting and overlaid. Cells above threshold were counted as positive, with the same threshold used for all brain regions. Brain necrosis, apoptosis, Bax and Bcl-2 immunohistochemistry findings are reported per mm^2 with each 40X HPF equating to 0.0359 mm^2.

Bax and Grp78 analysis with immunoblotting

Frozen caudal sections of the brain were put on dry ice and a cortical portion of gray matter was removed and homogenized in RIPA buffer supplemented with 1 mM NaV, 50 mM NaF, and 25 mM $C_3H_7O_6PNa_2XH2O$, and a protease inhibitor cocktail (Roche, Mississauga, ON). The solution was sonicated for 5 s, then mixed in a rotator for 10 min, and centrifuged at 300 × *g* for 15 min at 4 °C. The supernatant was collected and centrifuged at 16,000 × *g* for 20 min at 4 °C. The resulting supernatant was collected as the total cellular protein extract and quantified by colorimetric DC protein assay (BioRad Laboratories, Mississauga, ON). Loading samples were prepared with NuPAGE LDS Sample Buffer (4×) and Reducing Agent (10×) (Invitrogen Life Technologies Inc., Burlington, ON), and deionized water, and heated at 70 °C for 10 min to denature the proteins. Proteins (20μg/well) were separated by size via gel electrophoresis in gradient polyacrylamide gels (Novex, Thermo Scientific, Burlington, ON) and transferred onto polyvinylidenedifluoride membrane (Millipore). Male and female samples from each cohort (AGA-Control and FGR-MNR) were run on separate gels with the inclusion of a positive control (rat placenta) that had shown reactivity in a previous study using the same antibodies.[28] Membranes were blocked in 1× Tris-buffered saline-Tween 20 buffer with 5% non-fat milk, then probed using primary antibodies specific for the protein targets, Bax (rabbit monoclonal, 1:2000, sc-493, Santa Cruz Biotechnology, Santa Cruz, CA), Grp78 (mouse monoclonal, 1:300, sc-58774, Santa Cruz Biotechnology) and β-actin (mouse monoclonal, 1:50,000, A3854, Sigma-Aldrich Co., St Louis, MO), diluted in the blocking solution. Secondary antibodies were used to detect the species-specific portion of the primary antibody, donkey anti-rabbit IgG (1:10,000, 711-011-033, Jackson ImmunoResearch Laboratories, West Grove, PA) and donkey anti-mouse IgG (1:5000, 715-011-033, Jackson ImmunoResearch Laboratories), diluted in the blocking solution. Immuno-reactive bands were visualized using SuperSignal West Dura Chemiluminescent Substrate (Thermo Scientific, Nepean, ON). Protein bands underwent densitometry analysis using Image Lab 4.0 Software (BioRad Laboratories) normalized to β-actin as previously reported.[28] Bax and Grp78 protein levels normalized to the β-actin protein levels are presented as the mean change for FGR-MNR males from the AGA-Control males and FGR-MNR females from the AGA-Control females.

Data acquisition and statistical analysis

Fetal population characteristics, brain necrosis, apoptosis, and pro- and anti-apoptotic findings for the AGA-Control and FGR-MNR fetuses are presented as group means ± SEM. Population characteristics and brain findings were compared using two-way analysis of variance to determine the effects of MNR and sex. Where interactions between MNR and sex were present with $p < 0.05$, post hoc tests (Tukey) were carried out to determine the effect of MNR in males and females separately (Graphpad Software, San Diego, CA). For all analyses, statistical significance was assumed for $p < 0.05$.

Table 1. Fetal population characteristics

	Male		Female		*p* (ANOVA)		
	AGA-Control $N = 9$	FGR-MNR $N = 9$	AGA-Control $N = 9$	FGR-MNR $N = 9$	G	S	G × S
Fetal wt (g)	102 ± 3	62 ± 4	101 ± 3	64 ± 4	***	NS	NS
Brain wt (g)	2.76 ± 0.07	2.45 ± 0.09	2.72 ± 0.08	2.36 ± 0.07	**	NS	NS
Liver wt (g)	4.7 ± 0.2	2.6 ± 0.3	4.7 ± 0.4	2.7 ± 0.2	***	NS	NS
Brain/fetal wt (%)	2.70 ± 0.06	4.10 ± 0.25	2.72 ± 0.09	3.76 ± 0.16	***	NS	NS
Brain/liver wt	0.59 ± 0.02	1.01 ± 0.08	0.60 ± 0.05	0.90 ± 0.05	***	NS	NS
Placental wt (g)	7.4 ± 0.5	5.3 ± 0.5	6.7 ± 0.4	5.1 ± 0.4	**	NS	NS

AGA appropriate for gestational age, *FGR* fetal growth restricted, *MNR* maternal nutrient restricted, *G* group, *S* sex, *NS* not significant
Data presented as mean ± SEM; $^{**}p < .01$, $^{***}p < .001$

RESULTS

Fetal population characteristics

While 12 sows were bred under control conditions and 18 under MNR conditions, 3 animals from each of these groupings failed to become pregnant and 3 MNR animals delivered preterm. The remaining 9 control and 12 MNR animals had pregnancies continuing to necropsy at 60/61 days of gestation with 31 and 42 fetuses, respectively, whose body and placental weights have been reported.[10] The 80 g threshold for categorizing AGA and FGR fetal weights resulted in 20 AGA-Control fetuses and 25 FGR-MNR fetuses with the body, organ and placental weights from these animals also previously reported.[10] The 18 AGA-Control fetuses and 18 FGR-MNR fetuses presently studied were representative of the mean fetal weights from these select cohort groups with their population characteristics shown in Table 1. Changes in these population characteristics in the FGR-MNR fetuses from that of the AGA-Control fetuses were similar for both males and females. Briefly, FGR-MNR fetal weights were decreased ~38% while brain weights were decreased ~12%. Accordingly, the brain/fetal weight as a measure of brain sparing was increased ~45% in the FGR-MNR fetuses. FGR-MNR liver weights were decreased ~44%. Accordingly, the brain/liver weight as a measure of asymmetrical growth was increased ~60% in the FGR-MNR fetuses.

Necrotic and apoptotic appearing cells

The mean percentage of necrotic cells per mm^2 for the brain regions examined is shown in Table 2. Overall, very low levels of necrotic cells were observed across the brain regions, averaging 0.45% and 0.59% for the AGA-control and FGR-MNR animals, respectively, with no group or sex differences.

The mean number of TUNEL positive cells per mm^2 for the brain regions examined is shown in Table 3. While low levels of TUNEL positive cells were observed, these were higher in the male and female FGR-MNR animals compared to the male and female AGA-Control animals in the periventricular white matter, and the hippocampal CA1, CA4 and dentate gyrus. There additionally was a sex effect whereby TUNEL positive cells were increased in male AGA-Controls and FGR-MNRs compared to female AGA-controls and FGR-MNRs which was significant for all brain regions studied excepting the dentate gyrus.

Bax and Bcl-2 positive cell counts

Bax and Bcl-2 immunostaining were localized primarily within the cytosol and perinuclear membrane area as shown in the representative photomicrographs (Fig. 2), with the mean number of positive cells per mm^2 for the brain regions examined as shown in Table 4. While the number of Bax and Bcl-2 positive cells were not significantly changed between the animal groups for most brain regions, Bax positive cells were higher in the male and female FGR-MNRs compared to the male and female AGA-Controls in the hippocampal CA4, and Bcl-2 positive cells were lower in the male and female FGR-MNRs compared to the male and female AGA-Controls in the hippocampal dentate gyrus. There additionally were sex effects whereby Bcl-2 positive cells in male AGA-Controls and FGR-MNRs compared to female AGA-Controls and FGR-MNRs were decreased in the gray matter 4–5, but increased in the dentate gyrus and thalamus.

Table 2. Percent necrotic cells per mm^2

	Male		Female		*p* (ANOVA)		
	AGA-Control $N = 9$	FGR-MNR $N = 9$	AGA-Control $N = 9$	FGR-MNR $N = 9$	G	S	G×S
GM 2-3	0.1 ± 0.1	0.2 ± 0.1	0.1 ± 0.1	0.8 ± 0.6	NS	NS	NS
GM 4-5	0.4 ± 0.1	1.0 ± 0.4	0.7 ± 0.2	0.4 ± 0.2	NS	NS	NS
PVWM	0.0 ± 0.0	0.1 ± 0.1	0.0 ± 0.0	0.0 ± 0.0	NS	NS	NS
CA1	0.1 ± 0.1	0.3 ± 0.2	0.1 ± 0.1	0.1 ± 0.1	NS	NS	NS
CA4	1.6 ± 0.2	3.0 ± 0.8	2.5 ± 0.8	1.1 ± 0.4	NS	NS	NS
DG	0.4 ± 0.2	0.1 ± 0.1	0.1 ± 0.1	0.2 ± 0.2	NS	NS	NS
Thalamus	0.7 ± 0.2	0.8 ± 0.4	0.7 ± 0.2	0.5 ± 0.2	NS	NS	NS

AGA appropriate for gestational age, *FGR* fetal growth restricted, *MNR* maternal nutrient restricted, *G* group, *S* sex, *NS* not significant, *GM* gray matter, *PVWM* periventricular white matter, *DG* dentate gyrus
Data presented as mean ± SEM

The mean ratio of Bax to Bcl-2 positive cells was also assessed as a measure of pro-/anti- apoptotic activity with the findings shown in Fig. 3. While the Bax/Bcl-2 ratios were not significantly changed between the animal groups for most brain regions, these were higher in the male and female FGR-MNRs compared to the male and female AGA-Controls in the hippocampal CA4. There was also a sex effect in the thalamus whereby the Bax/Bcl-2 ratio was decreased in the male AGA-Controls and FGR-MNRs compared to female AGA-Controls and FGR-MNRs.

Bax and Grp78 protein levels

Bax was not changed by either group or sex for the brain tissue studied (Fig. 4). However, there was an interaction between group and sex for Grp78 whereby levels in the FGR-MNR females were increased by ~2.2-fold when compared to the AGA-Control females ($p < .05$), but with no significant change between the FGR-MNR males and AGA-Control males (Fig. 4).

DISCUSSION

FGR-MNR fetal weights were decreased ~38%, brain weights were decreased ~12%, and liver weights were decreased ~44%

Table 3. TUNEL positive cells per mm^2

	Male		Female		*p* (ANOVA)		
	AGA-Control $N = 9$	FGR-MNR $N = 9$	AGA-Control $N = 9$	FGR-MNR $N = 9$	G	S	G×S
GM 2-3	11.4 ± 2.2	18.1 ± 2.0	7.5 ± 1.7	7.2 ± 2.2	NS	**	NS
GM 4-5	16.7 ± 2.0	16.7 ± 4.5	7.0 ± 3.1	10.0 ± 2.8	NS	*	NS
PVWM	86 ± 15	142 ± 25	23 ± 5	75 ± 22	**	**	NS
CA1	4.7 ± 1.4	12.5 ± 2.3	0.6 ± 0.6	3.1 ± 1.4	**	***	NS
CA4	29.3 ± 6.1	43.2 ± 4.7	12.8 ± 3.3	25.3 ± 5.3	*	**	NS
DG	4.7 ± 1.4	12.5 ± 3.6	1.7 ± 1.1	7.2 ± 3.9	*	NS	NS
Thalamus	75 ± 10	84 ± 16	33 ± 6	36.8 ± 8.6	NS	***	NS

AGA appropriate for gestational age, *FGR* fetal growth restricted, *MNR* maternal nutrient restricted, *G* group, *S* sex, *NS* not significant, *GM* gray matter, *PVWM* periventricular white matter, *DG* dentate gyrus
Data presented as mean ± SEM; *$p < .05$, **$p < .01$, ***$p < .001$

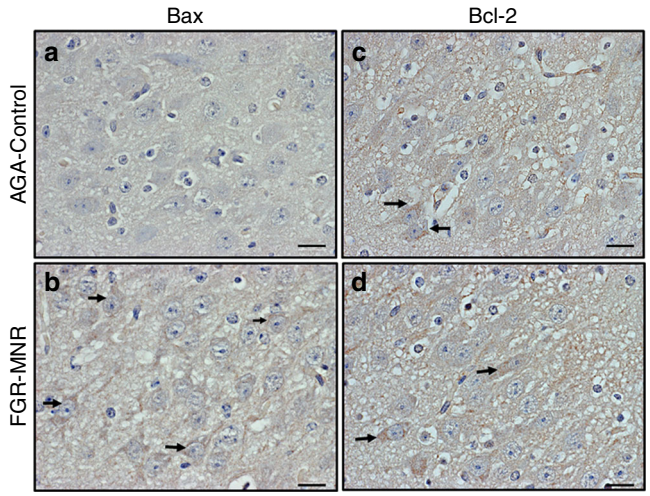

Fig. 2 Photomicrographs of Bax immunostaining in the CA4 of an AGA-Control (**a**) and FGR-MNR (**b**) fetus and Bcl-2 immunostaining in the CA4 of an AGA-Control (**c**) and FGR-MNR (**d**) fetus showing localization within the cytosol and perinuclear membrane area (immunoperoxidase, scale bar = 20μm). *AGA* appropriate for gestational age, *FGR* fetal growth restriction, *MNR* maternal nutrient restriction

compared to the AGA-Controls, indicating brain sparing and asymmetrical growth restriction. This is likely due in part to blood flow redistribution favoring the vital organs including the brain in response to chronic hypoxemia[29] which we have shown evidence for in the liver and kidneys of these FGR-MNR animals using immunoreactivity for Hypoxyprobe-1.[14] However, while increases in blood flow will lessen the fall in tissue oxygenation in the FGR brain, this is unlikely to be normalized when there is systemic hypoxemia.[29] As such, it is not surprising that FGR offspring in human and animal studies while showing brain sparing still have smaller brains and altered growth, whether due to placental insufficiency or maternal undernourishment when there is associated hypoxemia.[1,2,6–10,14,16,18,19,25,29]

Low levels of necrotic cells were seen in brain regions of the AGA-Controls using H&E morphology similar to that we[27] and others[30] have reported in studies of induced hypoxia in sheep. As such, it is possible that low levels of necrosis exist in the developing brain or, alternatively, are the result of processing artifacts and/or the inherent subjectivity of the scoring procedure.[31] However, despite the reduction in brain size in the FGR-MNR animals and presumed hypoxemia, there was no effect on measured levels of necrotic-appearing cells when compared to respective control group values. This would indicate that the threshold for energy depletion leading to membrane failure and structural cell damage has not been reached,[32] countered by the enactment of mechanisms to protect energy levels for membrane integrity by increasing brain blood flow and decreasing less essential energy usage as seen when tissue oxygenation is acutely limited.[33]

Apoptosis plays a central role during early brain development in post-mitotic cells coincident with neuronal differentiation and synaptogenesis with low levels normally seen.[34] Apoptosis in the fetal/neonatal brain can also be activated by chronic hypoxic insult leading to FGR and resulting in selective neuronal loss. However, most animal study has utilized mid to late pregnancy uterine artery ligation/ablation[1,7] placental embolization,[35] or maternal hypoxia[36–38] with the issue of initial hypoxia being later in onset and acutely induced. In the present study, TUNEL positive cells were found to be increased in the FGR-MNR animals in the periventricular white matter, and the hippocampal CA1, CA4, and dentate gyrus, when compared to that of the AGA-Controls. These findings with MNR-induced FGR, and the likelihood of early and gradual growth restriction in response to chronic hypoxia as well as nutrient deficiency, are similar to that observed with mid to late pregnancy hypoxia-induced FGR,[1,7,35–38] and again highlight the increased vulnerability of these brain areas to hypoxic insult whether acutely or chronically induced.[1,39]

TUNEL positive cells were also increased in male AGA-Controls and FGR-MNRs compared to female AGA-Controls and FGR-MNRs for all brain regions studied excepting the dentate gyrus. To our knowledge, sex differences for basal apoptotic activity during brain development have not been reported, although basal autophagy (by which cells degrade proteins and organelles) is increased in neonatal female rats compared to males.[40] This sex-related autophagy might protect against full-scale apoptosis during brain development by minimizing the accumulation in unfolded/misfolded proteins and associated initiation of pro-apoptotic events, thereby decreasing basal apoptotic activity in the female brain as herein noted. Alternatively, sex-dependent apoptotic pathways are known to exist in the neonatal brain whereby female cell death is predominantly triggered through caspase-dependent pathways, whereas male cell death is predominantly triggered through the poly(ADP-ribose) polymerase (PARP)-dependent pathway which is caspase-independent.[41,42] While this study of cell death has largely been in relation to acutely induced hypoxic-ischemic insult, these sex-dependent apoptotic pathways may also be utilized for basal apoptotic activity and be differentially activated during the brain's development thereby contributing to the differences seen between males and females. To our knowledge, sex differences for apoptotic activity in the FGR brain have likewise not been reported, and

Table 4. Bax and Bcl-2 positive cells per mm^2

		Male		Female		*p* (ANOVA)		
		AGA-Control $N = 9$	FGR-MNR $N = 9$	AGA-Control $N = 9$	FGR-MNR $N = 9$	G	S	G×S
GM 2-3	Bax	160 ± 26	193 ± 46	175 ± 26	153 ± 33	NS	NS	NS
	Bcl-2	424 ± 52	367 ± 61	352 ± 37	412 ± 33	NS	NS	NS
GM 4-5	Bax	47 ± 9	59 ± 18	71 ± 17	88 ± 17	NS	NS	NS
	Bcl-2	103 ± 19	104 ± 9	156 ± 11	159 ± 16	NS	**	NS
PVWM	Bax	52 ± 11	68 ± 23	65 ± 21	74 ± 14	NS	NS	NS
	Bcl-2	495 ± 73	412 ± 79	545 ± 71	400 ± 57	NS	NS	NS
CA1	Bax	431 ± 120	480 ± 105	441 ± 86	620 ± 172	NS	NS	NS
	Bcl-2	333 ± 83	500 ± 98	392 ± 117	437 ± 66	NS	NS	NS
CA4	Bax	38 ± 13	97 ± 40	26 ± 5	87 ± 19	**	NS	NS
	Bcl-2	86 ± 20	84 ± 16	83 ± 15	70 ± 7	NS	NS	NS
DG	Bax	134 ± 38	136 ± 42	139 ± 25	179 ± 38	NS	NS	NS
	Bcl-2	674 ± 175	469 ± 75	525 ± 95	252 ± 34	**	*	NS
Thalamus	Bax	5 ± 2	9 ± 4	11 ± 4	22 ± 7	NS	NS	NS
	Bcl-2	60 ± 12	91 ± 18	43 ± 3	55 ± 8	NS	*	NS

AGA appropriate for gestational age, *FGR* fetal growth restricted, *MNR* maternal nutrient restricted, *G* group, *S* sex, *NS* not significant, *GM* gray matter, *PVWM* periventricular white matter, *DG* dentate gyrus
Data presented as mean ± SEM; *$p < .05$, **$p < .01$

while increased in the male FGR-MNRs compared to the female FGR-MNRs, the incremental increase in TUNEL positive cells from basal levels was overall similar for both animal groups. This would suggest that the stimulus for increased apoptosis in the FGR brain is operating to a similar extent in both males and females, although it is of interest that increased oxidative stress which is known to occur with FGR[1,36,37,43] and can activate apoptotic pathways in the perinatal brain,[41,42] is more likely to do so through the PARP-dependent pathway predominant in males.

Bax and Bcl-2 play an important role in apoptotic cell death activation by regulating mitochondrial outer membrane permeabilization and effector protein release in response to apoptotic stimulae.[21,41] Accordingly, their expression has been studied in animal models with mid to late pregnancy hypoxia-induced FGR with Bax shown to be increased and Bcl-2 shown to be increased or decreased in the FGR brain, supporting the conjecture that these apoptotic regulators play a role in mediating the increased apoptosis with hypoxia-induced FGR.[1,7,36,37] In the present study, FGR-MNR animals showed increased Bax in the hippocampal CA4 with the Bax/Bcl-2 ratio also increased, and decreased Bcl-2 in the hippocampal dentate gyrus. These findings are qualitatively similar to that seen with late pregnancy hypoxia-induced FGR,[1,7,36,37] but the changes in Bax and Bcl-2 appear less pronounced possibly reflecting the insidious nature of MNR-induced FGR with slower onset and progression of related hypoxemia. Males from both cohort groups also showed decreased Bcl-2 in the gray matter 4–5 which would favor an increase in their TUNEL positive cells, and increased Bcl-2 in the hippocampal dentate gyrus and thalamus, which would favor a decrease in their TUNEL positive cells, none of which were observed. While indicating sex differences for Bax and Bcl-2 in the developing brain, the apparent discrepancy with apoptotic activity serves to highlight that there are other regulating proteins of apoptosis, and Bax and Bcl-2 may have functions beyond their role in regulating cellular apoptosis during the brain's development.[7,21,36,41,42]

Protein expression in cortical gray matter for Bax and Grp78 was also assessed by western blot analysis to complement the IHC findings. Bax protein levels were unchanged in the FGR-MNRs from that of the AGA-Controls and between males and females which is consistent with the IHC findings in the gray matter layers 2–3 and 4–5. However, Grp78 protein levels were increased in the FGR-MNRs from that of the AGA-Controls, but only in females. This finding is notable since Grp78 is increased to promote protein folding when there is an accumulation of unfolded/misfolded proteins with hypoxic-related oxidative stress[23,24] which might be occurring with MNR-induced FGR given the evidence for chronic hypoxia.[14] Moreover, this increase in Grp78 would serve to blunt the associated pro-apoptotic cascade seen with unfolded/misfolded proteins[23,24] and could thereby contribute to the lowering of TUNEL positive cells in the FGR brains of the females compared to the males.

MNR-induced FGR as studied resulted in brain sparing but with brains still smaller, analogous to the human situation with early-onset FGR.[1,2,19] Cell death from necrosis remained unchanged in the FGR brains indicating that energy levels for membrane integrity have been maintained. Conversely, cell death from apoptosis was increased in the periventricular white matter and the hippocampal areas in the FGR brains highlighting increased vulnerability with hypoxic-related FGR whether resulting from maternal undernourishment or placental insufficiency, and contributing to their reduction in size as reported clinically.[1,2,39] Basal and FGR-related apoptotic activity was also increased in males for most brain areas studied that may involve sex-dependent differences in basal autophagy and/or apoptotic pathways as discussed.[40–42] Changes in Bax and Bcl-2 expression supported a role in the increased apoptosis seen in some of the brain areas, but not others, which may be attributed to the insidious nature of MNR-induced FGR and the role of other regulating proteins of apoptosis that have not been assessed.[7,21,36,41,42] Lastly, Grp78 expression was increased in the cortical gray matter of the FGR females implicating an accumulation of unfolded/misfolded proteins resulting from hypoxic-related oxidative stress[23,24,36,37] which is likely to occur with MNR-induced FGR.[1,14,36,37] While accumulation of unfolded/misfolded proteins is also likely in FGR males, the absence of any change in Grp78 expression to ameliorate the pro-apoptotic cascade with unfolded/misfolded proteins is another example whereby females show better adaptation to hypoxia and for the brain, decreases the risk for later neurological adversity compared to males.[1,12] Importantly,

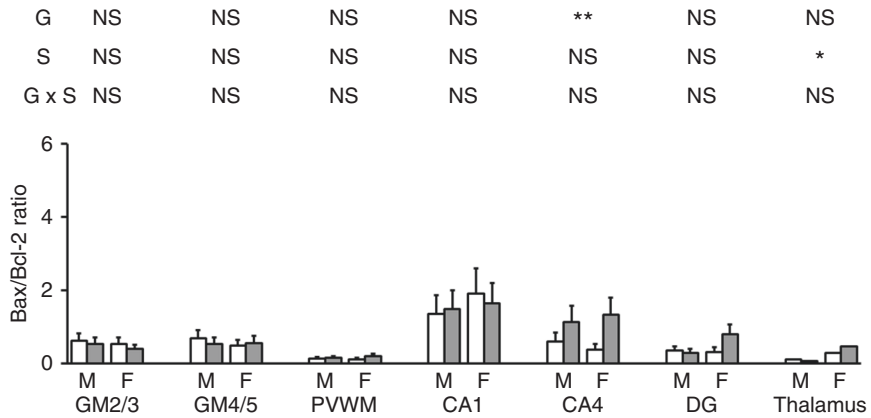

Fig. 3 Bax to Bcl-2 positive cell ratios in the brain regions of the male and female AGA-Control fetuses (open bars, $n = 9$ and 9) and male and female FGR-MNR fetuses (gray bars, $n = 9$ and 9). Data presented as mean ± SEM; *$p < .05$, **$p < .01$. *AGA* appropriate for gestational age, *FGR* fetal growth restriction, *MNR* maternal nutrient restriction, *G* group, *S* sex, *GM* gray matter, *PVWM* periventricular white matter, *DG* dentate gyrus

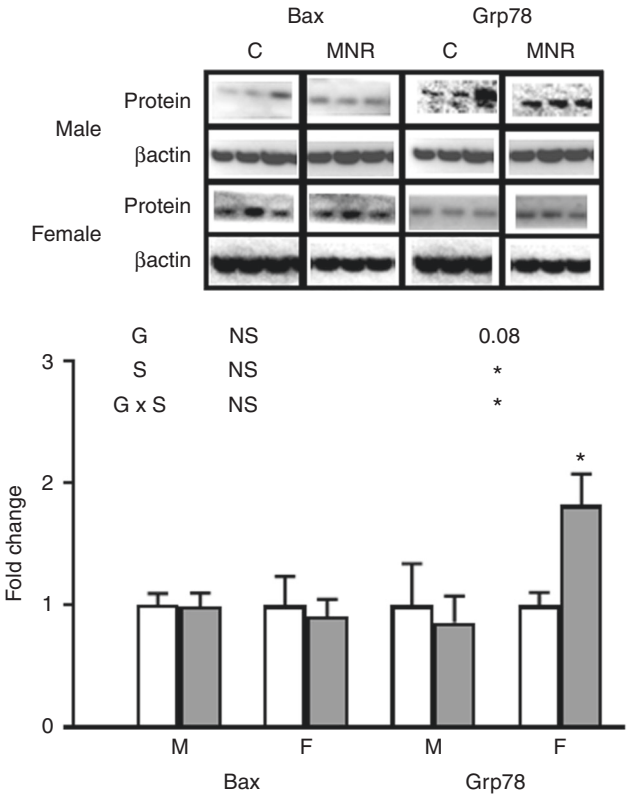

Fig. 4 Bax and Grp78 protein expression in the gray matter. Representative immunoblots from male and female AGA-Control and FGR-MNR fetuses are displayed. Density of Bax and Grp78 normalized to β-actin and presented as the mean fold change ± SEM in male and female FGR-MNR fetuses (gray bars, $n = 8$ and 8) compared with male and female AGA-Control fetuses (open bars, $n = 7$ and 7). *$p < .05$, *AGA* appropriate for gestational age, *FGR* fetal growth restriction, *MNR* maternal nutrient restriction, *G* group, *S* sex

the findings reported provide further insight into the brain's developmental adaptations with moderate/severe FGR whether resulting from maternal undernourishment or placental insufficiency, to the extent that both involve aberrant placental development with chronic hypoxia and nutrient deficiency as primary signaling mechanisms.[1–3,10,14,15,18]

ACKNOWLEDGEMENTS

We thank Dr Lin Zhao for support with the protein analysis, and Ms Jennifer Ryder for assistance with the manuscript. Supported by grants from the Children's Health Research Institute and Department of Obstetrics and Gynecology, The University of Western Ontario, London, Canada (B.S.R., R.H.)

AUTHOR CONTRIBUTIONS

The authors contributed to all three aspects of the *Pediatric Research* criteria.

ADDITIONAL INFORMATION

Competing interests: B.S.R. is the recipient of a Canada Research Chair Tier 1 in Fetal and Neonatal Health and Development. All the remaining authors declare no competing interests.

Publisher's note: Springer Nature remains neutral with regard to jurisdictional claims in published maps and institutional affiliations.

REFERENCES

1. Miller, S. L., Huppi, P. S. & Mallard, C. The consequences of fetal growth restriction on brain structure and neurodevelopmental outcome. *J. Physiol.* **594**, 807–823 (2016).
2. Malhotra, A. et al. Detection and assessment of brain injury in the growth-restricted fetus and neonate. *Pediatr. Res.* **82**, 184–193 (2017).
3. Resnick, R. & Creasy, R. K. in *Maternal-Fetal Medicine* 7th edn (eds Creasy, R. K. et al.) pp. 743–755 (Elsevier Sauders, Philadelphia, PA, 2014).
4. Grantham-McGregor, S. & Baker-Henningham, H. Review of the evidence linking protein and energy to mental development. *Public Health Nutr.* **8**(7A), 1191–1201 (2005).
5. Crozier, S. R., Robinson, S. M., Godfrey, K. M., Cooper, C. & Inskip, H. M. Women's dietary patterns change little from before to during pregnancy. *J. Nutr.* **139**, 1956–1963 (2009).
6. Rees, S., Harding, R. & Walker, D. An adverse intrauterine environment: implications for injury and altered development of the brain. *Int. J. Dev. Neurosci.* **26**, 3–11 (2008).
7. Basilious, A., Yager, J. & Fehlings, M. G. Neurological outcomes of animal models of uterine artery ligation and relevance to human intrauterine growth restriction: a systematic review. *Dev. Med. Child Neurol.* **57**, 420–430 (2015).
8. Lafeber, H. N., Rolph, T. P. & Jones, C. T. Studies on the growth of the fetal guinea pig. The effects of ligation of the uterine artery on organ growth and development. *J. Dev. Physiol.* **6**, 441–459 (1984).
9. Turner, A. J. & Trudinger, B. J. A modification of the uterine artery restriction technique in the guinea pig fetus produces asymmetrical ultrasound growth. *Placenta* **30**, 236–240 (2009).
10. Elias, A. A., Ghaly, A., Matushewski, B., Regnault, T. R. & Richardson, B. S. Maternal nutrient restriction in guinea pigs as an animal model for inducing fetal growth restriction. *Reprod. Sci.* **23**, 219–227 (2016).

11. McCarthy, M. M., Arnold, A. P., Ball, G. F., Blaustein, J. D. & De Vries, G. J. Sex differences in the brain: the not so inconvenient truth. *J. Neurosci.* **32**, 2241–2247 (2012).
12. Bao, A. M. & Swaab, D. F. Sex differences in the brain, behavior, and neuropsychiatric disorders. *Neuroscientist* **16**, 550–565 (2010).
13. Carter, A. M. Animal models of human placentation-a review. *Placenta* **28**(Suppl A), S41–S47 (2007).
14. Elias, A. A. et al. Maternal nutrient restriction in guinea pigs leads to fetal growth restriction with evidence for chronic hypoxia. *Pediatr. Res.* **82**, 141–147 (2017).
15. Roberts, C. T. et al. Maternal food restriction reduces the exchange surface area and increases the barrier thickness of the placenta in the guinea-pig. *Placenta* **22**, 177–185 (2001).
16. Kind, K. L. et al. Chronic maternal feed restriction impairs growth but increases adiposity of the fetal guinea pig. *Am. J. Physiol. Regul. Integr. Comp. Physiol.* **288**, R119–R126 (2005).
17. Nevin, C. L. et al. Maternal nutrient restriction in guinea pigs as an animal model for studying growth-restricted offspring with postnatal catch-up growth. *Am. J. Physiol. Regul. Integr. Comp. Physiol.* **314**, R647–R654 (2018).
18. Economides, D. L. & Nicolaides, K. H. Blood glucose and oxygen tension levels in small-for-gestational-age fetuses. *Am. J. Obstet. Gynecol.* **160**, 385–389 (1989).
19. Kramer, M. S. et al. Determinants of fetal growth and body proportionality. *Pediatrics* **86**, 18–26 (1990).
20. Godfrey, K. & Robinson, S. Maternal nutrition, placental growth and fetal programming. *Proc. Nutr. Soc.* **57**, 105–111 (1998).
21. Banasiak, K. J., Xia, Y. & Haddad, G. G. Mechanisms underlying hypoxia-induced neuronal apoptosis. *Prog. Neurobiol.* **62**, 215–249 (2000).
22. Scott, R. J. & Hegyi, L. Cell death in perinatal hypoxic-ischaemic brain injury. *Neuropathol. Appl. Neurobiol.* **23**, 307–314 (1997).
23. Liu, D., Zhang, M. & Yin, H. Signaling pathways involved in endoplasmic reticulum stress-induced neuronal apoptosis. *Int. J. Neurosci.* **123**, 155–162 (2013).
24. Lee, A. S. The ER chaperone and signaling regulator GRP78/BiP as a monitor of endoplasmic reticulum stress. *Methods* **35**, 373–381 (2005).
25. Piorkowska, K. et al. Synaptic development and neuronal myelination are altered with growth restriction in fetal Guinea pigs. *Dev. Neurosci.* **36**, 465–476 (2014).
26. Jansson, T. & Persson, E. Placental transfer of glucose and amino acids in intrauterine growth retardation: studies with substrate analogs in the awake guinea pig. *Pediatr. Res.* **28**, 203–208 (1990).
27. Rocha, E., Hammond, R. & Richardson, B. Necrotic cell injury in the preterm and near-term ovine fetal brain after intermittent umbilical cord occlusion. *Am. J. Obstet. Gynecol.* **191**, 488–496 (2004).
28. Wong, M. K., Nicholson, C. J., Holloway, A. C. & Hardy, D. B. Maternal nicotine exposure leads to impaired disulfide bond formation and augmented endoplasmic reticulum stress in the rat placenta. *PLoS ONE* **10**, e0122295 (2015).
29. Richardson, B. S. in *Clinics in Perinatology* (ed. Manning, F.) pp. 595–611 (WB Saunders Co., Philadelphia, 1989).
30. Keunen, H., Blanco, C. E., van Reempts, J. L. & Hasaart, T. H. Absence of neuronal damage after umbilical cord occlusion of 10, 15, and 20 min in midgestation fetal sheep. *Am. J. Obstet. Gynecol.* **176**, 515–520 (1997).
31. Schmued, L. C., Albertson, C. & Slikker, W. Jr. Fluoro-Jade: a novel fluorochrome for the sensitive and reliable histochemical localization of neuronal degeneration. *Brain Res.* **751**, 37–46 (1997).
32. Astrup, J. Energy-requiring cell functions in the ischemic brain. Their critical supply and possible inhibition in protective therapy. *J. Neurosurg.* **56**, 482–497 (1982).
33. Kaneko, M., White, S., Homan, J. & Richardson, B. Cerebral blood flow and metabolism in relation to electrocortical activity with severe umbilical cord occlusion in the near-term ovine fetus. *Am. J. Obstet. Gynecol.* **188**, 961–972 (2003).
34. Blaschke, A. J., Staley, K. & Chun, J. Widespread programmed cell death in proliferative and postmitotic regions of the fetal cerebral cortex. *Development* **122**, 1165–1174 (1996).
35. Duncan, J. R., Cock, M. L., Harding, R. & Rees, S. M. Relation between damage to the placenta and the fetal brain after late-gestation placental embolization and fetal growth restriction in sheep. *Am. J. Obstet. Gynecol.* **183**, 1013–1022 (2000).
36. Guo, R. et al. Brain injury caused by chronic fetal hypoxemia is mediated by inflammatory cascade activation. *Reprod. Sci.* **17**, 540–548 (2010).
37. Dong, Y. et al. Chronic fetal hypoxia produces selective brain injury associated with altered nitric oxide synthases. *Am. J. Obstet. Gynecol.* **204**, 254.e16–28 (2011).
38. Evans, L. C., Liu, H. & Thompson, L. P. Differential effect of intrauterine hypoxia on caspase 3 and DNA fragmentation in fetal guinea pig hearts and brains. *Reprod. Sci.* **19**, 298–305 (2012).
39. Mallard, E. C., Williams, C. E., Johnston, B. M. & Gluckman, P. D. Increased vulnerability to neuronal damage after umbilical cord occlusion in fetal sheep with advancing gestation. *Am. J. Obstet. Gynecol.* **170**(1 Pt 1), 206–214 (1994).
40. Weis, S. N. et al. Autophagy in the brain of neonates following hypoxia-ischemia shows sex- and region-specific effects. *Neuroscience* **256**, 201–209 (2014).
41. Renolleau, S., Fau, S. & Charriaut-Marlangue, C. Gender-related differences in apoptotic pathways after neonatal cerebral ischemia. *Neuroscientist* **14**, 46–52 (2008).
42. Charriaut-Marlangue, C., Besson, V. C. & Baud, O. Sexually dimorphic outcomes after neonatal stroke and hypoxia-ischemia. *Int J. Mol. Sci.* **19**, pii: E61 (2017).
43. Hracsko, Z., Orvos, H., Novak, Z., Pal, A. & Varga, I. S. Evaluation of oxidative stress markers in neonates with intra-uterine growth retardation. *Redox Rep.* **13**, 11–16 (2008).